Biochimica et Biophysica Acta 1848 (2015) 1147–1156

Contents lists available at ScienceDirect

Biochimica et Biophysica Acta

journal homepage: www.elsevier.com/locate/bbamem

Interaction of a peptide derived from C-terminus of human TRPA1 channel with model membranes mimicking the inner leaflet of the plasma membrane

Katja Witschas [a,b], Marie-Lise Jobin [a], Dursun Nizam Korkut [c], Maria Magdalena Vladan [a], Gilmar Salgado [c], Sophie Lecomte [a], Viktorie Vlachova [b], Isabel D. Alves [a,*]

[a] CBMN-UMR 5248 CNRS, University of Bordeaux, IPB, Allée Geoffroy St. Hilaire, 33600 Pessac, France
[b] Department of Cellular Neurophysiology, Institute of Physiology, Academy of Sciences of the Czech Republic, Videnska 1083, 142 20 Prague 4, Czech Republic
[c] INSERM, U869, ARNA Laboratory, University of Bordeaux, 2 rue Robert Escarpit, 33607 Pessac, France

ARTICLE INFO

Article history:
Received 10 November 2014
Received in revised form 21 January 2015
Accepted 4 February 2015
Available online 14 February 2015

Keywords:
TRP channels
Peptide–lipid interactions
Secondary structure
Conformation
Lipid-selective interaction

ABSTRACT

The transient receptor potential ankyrin 1 channel (TRPA1) belongs to the TRP cation channel superfamily that responds to a panoply of stimuli such as changes in temperature, calcium levels, reactive oxygen and nitrogen species and lipid mediators among others. The TRP superfamily has been implicated in diverse pathological states including neurodegenerative disorders, kidney diseases, inflammation, pain and cancer. The intracellular C-terminus is an important regulator of TRP channel activity. Studies with this and other TRP superfamily members have shown that the C-terminus association with lipid bilayer alters channel sensitivity and activation, especially interactions occurring through basic residues. Nevertheless, it is not yet clear how this process takes place and which regions in the C-terminus would be responsible for such membrane recognition. With that in mind, herein the first putative membrane interacting region of the C-terminus of human TRPA1, (corresponding to a 29 residue peptide, IAEVQKHASLKRIAMQVELHTSLEKKLPL) named H1 due to its potential helical character was chosen for studies of membrane interaction.
The affinity of H1 to lipid membranes, H1 structural changes occurring upon this interaction as well as effects of this interaction in lipid organization and integrity were investigated using a biophysical approach. Lipid models systems composed of zwitterionic and anionic lipids, namely those present in the lipid membrane inner leaflet, where H1 is prone to interact, where used. The study reveals a strong interaction and affinity of H1 as well as peptide structuration especially with membranes containing anionic lipids. Moreover, the interactions and peptide structure adoption are headgroup specific.

1. Introduction

The TRP superfamily comprises a large group of non-selective cation channels. They respond to diverse stimuli such as temperature, pressure, osmolarity, pH, and various chemical compounds including plant ingredients [1,2]. Moreover, TRP channel activity is modulated by calcium ions and lipid metabolites [3,4]. TRP ion channels are widely expressed in many different tissues and cell types, where they are implicated in diverse pathological states, including neurodegenerative disorders, kidney diseases, inflammation, pain and cancer [5,6]. TRP channels are organized into six families: classical (TRPC), vanilloid (TRPV), melastatin (TRPM), muclopins (TRPML), polycystin (TRPP), and ankyrin (TRPA). Similarly to voltage-gated potassium channels, TRP channels have four subunits, consisting of six transmembrane segments (S1–S6) each, a pore region loop between S5 and S6 segment, and long cytosolic N- and C-termini.

The transient receptor potential ankyrin 1 channel (TRPA1) is a nociceptor and polymodal ion channel activated by deep cooling (<17 °C), depolarizing voltages, calcium ions, environmental irritants (such as allyl isothiocyanate from wasabi), endogenous mediators involved in inflammation (including bradykinin), reactive oxygen and nitrogen species, and lipid metabolites (such as arachidonic acid) [7,8]. Furthermore, TRPA1 is regulated by phosphatidylinositol-4,5-

Abbreviations: ATR-FTIR, attenuated total reflection Fourier transform infrared; CD, circular dichroism; DMPA, dimyristoyl phosphatidic acid; DMPC, dimyristoyl phosphatidylcholine; DMPG, dimyristoyl phosphatidyglycerol; DMPS, dimyristoyl phosphatidylserine; DSC, differential scanning calorimetry; LUV, large unilamellar vesicle; MLV, multilamellar vesicle; NMR, nuclear magnetic resonance; P/L, peptide/lipid ratio; PI(4,5)P_2, L-α-phosphatidylinositol-4,5-bisphosphate; POPA, palmitoyl-oleoyl-phosphatidic acid; POPC, palmitoyl-oleoyl-phosphatidylcholine; POPE, palmitoyl-oleoyl-phosphatidylethanolamine; POPG, palmitoyl-oleoyl-phosphatidylglycerol; POPS, palmitoyl-oleoyl-phosphatidylserine; DPC, 1,2-di-0-dodecyl-*sn*-glycero-3-phosphocholine; SDS, sodium dodecyl sulfate; PWR, plasmon waveguide resonance; SUVs, small unilamellar vesicles

* Corresponding author at: Institute of Chemistry & Biology of Membranes & Nanoobjects (UMR5248 CBMN), CNRS – Université de Bordeaux – Institut Polytechnique Bordeaux, All. Geoffroy Saint-Hilaire 33600 Pessac, France. Tel.: +33 540006849.
E-mail address: i.alves@cbmn.u-bordeaux.fr (I.D. Alves).

http://dx.doi.org/10.1016/j.bbamem.2015.02.003
0005-2736/

bisphosphate (PIP_2), yet the PIP_2 binding sites have not been determined [9–11].

The specific binding of anionic lipids to certain protein domains is emerging as an important mechanism of channel regulation [12,13]. It is thought that distinct positively charged side chains from the protein interact with negatively charged lipid headgroups. Interactions between nontransmembrane protein domains and the lipid membrane were proposed to modulate ion channel activity [14–16]. The intracellular C-terminus is an important regulator of TRP channel activity [17–19]. Positively charged residues at the C-terminus of TRP channels have been shown to be putative PIP_2 interacting sites [20–22]. For the heat and capsaicin receptor TRPV1, it has been demonstrated that association of the C-terminus with the lipid bilayer alters channel sensitivity to thermal and chemical stimuli [23]. Besides phosphoinositides, several other negatively charged intracellular lipids, including phosphatidylglycerol, were reported to support TRPV1 activity [24].

Negatively charged molecules present in the inner leaflet of the cell membrane such as polyphosphates and phosphoinositides regulate TRPA1 from the cytoplasmic side, probably through interaction with positively charged domains in the C-terminus [25]. Electrophysiological studies show that basic amino acid residues in the C-terminus of the pain and wasabi receptor TRPA1 play a vital role in activation behavior and chemical sensitivity of the ion channel protein [25]. Therefore, it is likely that the basic residues in the C-terminus of TRPA1 may participate in channel–lipid interactions. Such polybasic clusters may be able to specifically recognize negatively charged phospholipids, and to associate with the membrane to control channel gating.

Following these thoughts, herein we propose to investigate the potential of the C-terminal region of the TRPA1 channel for membrane interaction. Since the C-terminal is extremely long (162 residues), we have made a search for potential membrane interacting sequences within this region. Taking into account that the interaction between the TRPA1 channel and the membrane are postulated to occur through positively charged amino acid residues, by the establishment of electrostatic interactions with anionic lipids, databases to predict antimicrobial peptide activity were used. Thus, we employed a web server-based method for predicting antibacterial peptides in a protein sequence to identify regions in the C-terminus of human TRPA1 with a high propensity for interaction with negatively charged phospholipids [26]. Indeed, antimicrobial peptides, despite their great diversity with respect to their amino acid sequence and secondary structure, they share as a common feature an affinity for negatively charged phospholipids [26]. An important property of antimicrobial peptides is their capability to distinguish bacterial from mammalian cells based on the differences in plasma membrane lipid composition [27]. In mammalian cells, the outer leaflet of the plasma membrane is composed of zwitterionic lipids, whereas substantial amounts of negatively charged phospholipids are present on the inner (cytosolic) leaflet of the plasma membrane [28,29]. In contrast, anionic lipids exposed on the outside of the bacterial membrane govern cell selectivity of antimicrobial peptides [30]. We have chosen the first membrane-interacting sequence in the C-terminus region of TRPA1 channel as potential site of interaction with the inner lipid leaflet of the membrane. This corresponds to a peptide of 29 amino acid residues (IAEVQKHASLKRIAMQVELHTSLEKKLPL) harboring 5 positively charged residues and 13 hydrophobic ones, named H1 due to its predicted helical propensity. To investigate the potential interaction of H1 with the cell membrane inner leaflet, we have employed lipid model systems containing anionic lipids (some of which present in the membrane inner leaflet like PIP_2, phosphatidylserine, phosphatidic acid). The interaction and structural changes induced by H1 in the lipid systems were monitored using several biophysical techniques. The possible functional role of Ca^{2+} in membrane association and structural characteristics of the peptide was studied. Results show that the peptide strongly binds to anionic lipids (dissociation constants in the nM range) present in the inner leaflet of eukaryotic plasma membranes. An enhanced affinity was observed in the case of PS. Calorimetry (differential scanning calorimetry) and plasmon waveguide resonance (PWR) reveal that peptide influence on lipid organization and packing is highly dependent on the lipid composition. Higher membrane affinity was observed in the presence of PS and PIP_2. As per the peptide structural changes upon lipid interaction, it was observed that H1 partially folds into β-sheet structure in the presence of anionic lipids and in a headgroup-specific manner. Therefore the first membrane-proximal cluster of positively charged residues in the cytoplasmic C-terminus of TRPA1 is implicated in protein–lipid interactions governed by electrostatic forces and lipid specificity akin to those found for other membrane-active peptides with cell membranes.

2. Materials and methods

2.1. Materials

All lipids were purchased from Avanti Polar Lipids (Alabaster, AL). Calcein was obtained from Sigma. The peptide (H1, IAEVQKHASLKRIAMQVELHTSLEKKLPL) was purchased from Selleckchem (Houston, TX) and used without further purification.

2.2. Preparation of MLVs and LUVs

Liposomes were prepared by dissolving the appropriate amounts of lipid into chloroform or a mixture of chloroform and methanol 2/1 (v/v), followed by solvent evaporation under nitrogen to deposit the lipid as a film on the wall of a test tube. Final traces of solvent were removed in a vacuum chamber attached to a liquid nitrogen trap during 3–4 h. Dried lipid films were hydrated with 10 mM Tris, 0.1 M NaCl, 2 mM EDTA, pH 7.6 (Tris buffer) (for DSC experiments) or with 10 mM phosphate buffer, pH 7.6 (for CD experiments) and thoroughly vortexed at a temperature superior to the phase transition temperature (Tm) of the lipid to obtain MLVs. To better mimic biological conditions, the peptide was added to the lipids after vesicle/liposome formation. To form LUVs, the MLV dispersion was subjected to five freeze/thawing cycles and passed 11 times through a mini-extruder equipped with two stacked 0.1 μm polycarbonate filters (Avanti, Alabaster, AL).

2.3. Calcein leakage

Calcein leakage assays are a quick and simple method to test lipid membrane integrity upon peptide action. While liposome encapsulated calcein is not fluorescent, perturbations in membrane integrity by peptides (e.g. pore formation) result in a fluorescence increase. Calcein-containing LUVs were prepared using the same protocol used to make regular LUVs, except for the hydration step of the lipid films performed in presence of 70 mM calcein. Free calcein was separated from calcein-containing LUVs using size exclusion column chromatography (Sephadex G-75) with Tris as elution buffer. The concentration of lipids was estimated using Rouser protocol [31]. For the assay, the lipid concentration was set at 1 μM and a P/L ratio of 1/50 and 1/25 used. All measurements were performed with a Perkin Elmer LS55 spectrometer (Buckinghamshire, UK). Data were collected every 1 s at room temperature using a $\lambda_{exc} = 485$ nm and $\lambda_{em} = 515$ nm with an emission and excitation slit of 2.5 nm in a cuvette of 2 mL. The fluorescence from calcein at 70 mM concentration was low due to self-quenching, but increased considerably upon dilution. The fluorescence intensity at equilibrium was measured after 2.5 h. At the end of the assay, complete leakage of LUVs was achieved by adding 100 μL of 10% Triton X-100 solution dissolving the lipid membrane without interfering with the fluorescence signal. The percentage of calcein release was calculated according to the following equation:

$$\%\text{Calcein leakage} = (F_t - F_o)/(F_f - F_o) * 100 \quad (1)$$

where the percent of calcein leakage is the fraction of dye released (normalized membrane leakage), F_t is the measured fluorescence intensity at time t, and F_o and F_f are the fluorescence intensities at times $t = 0$, and after final addition of Triton X-100, respectively. A dilution correction was applied on the fluorescence intensity after injection of the Triton X-100.

2.4. Differential scanning calorimetry

DSC experiments provide information about the thermodynamics of lipid phase changes within membranes. By following the effect of the peptide on the lipid phase transition properties (temperature, enthalpy, cooperativity of the transition, etc), one can determine whether the peptide interacts and inserts into the lipid fatty acid chains and whether it affects the lipid fluidity. When applied to binary lipid mixtures additional information can be obtained as further described in the results section. Microcalorimetry experiments were performed with a Nano DSC-II microcalorimeter (CSC) driven by a DSC-run software. The peptide was gradually added to the same sample of lipid MLVs to obtain peptide/lipid molar ratios of 1/100, 1/50 and 1/25. The total lipid concentration used was 1 mg/mL (ca. 1.45 mM) for the single lipids and 6 mg/mL (ca. 8.9 mM) for the binary lipid mixtures. For each peptide concentration, a minimum of four heating and four cooling scans were performed. A scan rate of 1 °C/min was used and there was a delay of 10 min between sequential scans in a series to allow thermal equilibration. A scan of the peptide alone dissolved in buffer at peptide concentrations corresponding to those at the higher P/L studied (1/10), exhibited no thermal events over the temperature range of 0–80 °C. This indicates that endothermic events observed in the presence of lipid arise solely from phase transitions of the phospholipids vesicles. Data analysis was performed by the fitting program CPCALC provided by CSC.

2.5. Circular dichroism

CD experiments were performed both on the H1 peptide in solution and in contact with liposomes of varied lipid composition. With this method the secondary structure of the peptide is obtained, and one can determine whether the lipid contact changes the peptide structure. CD data was recorded on a Jasco J-815 CD spectrophotometer with a 1 mm path length. Far-UV spectra were recorded from 185 or 195 to 250 nm with a 0.5 nm step resolution and a 1 nm bandwidth at 300 K. The scan speed was 50 nm/min (1 s response time), and the spectra were averaged over 7 scans. CD spectra were collected for peptide samples in a 10 mM phosphate buffer at concentrations varying from 20 to 120 μM for the peptide alone and in presence of the lipid whose concentration was 1250 μM (P/L ratios investigated ranged from 1/100 to 1/10). Measurements with different DPC/SDS molar ratios mixed micelle (9/1, 4/1, 1/1) as well as SDS alone were also acquired. For each sample, the background (buffer or liposome/micelle in absence of peptide) was automatically subtracted from the signal. Spectra were smoothed using a Savitzky–Golay smoothing filter and data are reported as $\Delta\varepsilon$ (M^{-1} cm^{-1}). Spectra deconvolution is performed using CDFriend, a software developed by S. Buchoux (unpublished). Like CDNN, CDpro and other tools, this program allows the determination of the secondary structure content of peptides and proteins based reference protein structures from a database.

2.6. Plasmon waveguide resonance (PWR) spectroscopy

PWR provides information about the affinity (from the pM to mM) and kinetics (in the msec) of molecular interactions in real time, directly (no labeling needed) and with high sensitivity (down to femtomole quantities of material). When applied to anisotropic oriented objects such as the case of lipid membranes it can also provide structural information (anisotropy, membrane thickness). PWR experiments were performed on a beta PWR instrument from Proterion Corp. (Piscataway, NJ) that had a spectral angular resolution of 1 mdeg. Resonances can be obtained with light whose electric vector is either parallel (*s*-polarization) or perpendicular (*p*-polarization) to the plane of the resonator surface. The principles behind the technique and information obtained have been reported and will not be developed here (as example refer to [32–34]). The sample to be analyzed (a lipid bilayer membrane) was immobilized on the resonator surface and placed in contact with an aqueous medium (10 mM Tris–HCl pH 7.6, 100 mM NaCl), into which the H1 peptide is then introduced. The self-assembled lipid bilayer was formed using a solution (in butanol/squalene, 0.93:0.07, v/v) of 8 mg/mL of lipid (Avanti Polar Lipids). The method used to prepare the lipid bilayer is based in on the procedure by Mueller and Rudin [35] to make black lipid membranes across a small hole in a Teflon block, the method has been reported [36,37]. After bilayer formation, H1 peptide is incrementally added to the cell sample compartment and the spectral changes monitored with both polarizations. Affinities between the peptide and the lipids were obtained by plotting the PWR spectral changes that occur upon incremental additions of ligand to the cell. Data fitting (GraphPad Prism) through a hyperbolic saturation curve provides the dissociation constants. It should be noted that concomitantly with the binding process other processes such as membrane reorganization and solvation occur and thus the dissociation constants correspond to apparent dissociation constants.

2.7. Attenuated total reflexion infrared spectroscopy

Polarized ATR-FTIR provides information about the secondary structure of peptides and their orientation in contact with lipid membranes. Additionally, information about the effect in the lipid ordering and hydration can be obtained. Spectra were recorded on a Nicolet 6700 FT-IR spectrometer (Nicolet Instrument, Madison,WI) equipped with a liquid nitrogen cooled mercury–cadmium–telluride detector (ThermoFisher Scientific, San Jose, CA, USA), with a spectral resolution of 4 cm^{-1} and a one-level zero filling.

Lipid bilayers adsorbed on a germanium ATR crystal were obtained by spontaneous fusion of small unilamellar vesicles (SUV) of pure POPC or a mixture of POPC with anionic lipids. The total lipid concentration used was 1.5 mg/mL (ca. 1.96 mM). SUV were prepared by tip sonication for 30 min after direct hydration of lipid films by D_2O buffer containing 0.1 M of NaCl. After bilayer formation at the crystal surface, the excess of SUV was removed by a buffer solution in D_2O. Since ATR spectroscopy is sensitive to the orientation of the lipid and peptide [38], spectra were recorded with a parallel (p) and perpendicular (s) polarization of the incident light. All the orientation information is then contained in the dichroic ratio $R_{ATR} = Ap/As$, where Ap and As represent the absorbance of the considered band for the p or s polarization of the incident light, respectively (for more details see [39]). H1 peptide at 1 mM was incubated for 10 min with the bilayer, the non-interacting peptide was removed by washing three times with D_2O.

2.8. Nuclear magnetic resonance spectroscopy

Two samples of peptide H1 (IAEVQKHASLKRIAMQVELHTSLEKKLPL) were prepared: one in 10 mM phosphate buffer with 50 mM NaCl at pH 6.8 solution and one in a membrane mimicking interface composed of deuterated DPC/SDS 9/1 (mol/mol) mixed micelle (Avanti® Polar Lipids) in the previously mentioned buffer. The sample in aqueous solution is prepared by dissolving 1.2 mg of peptide H1 in buffer and 10% (v/v) D_2O for a total volume of 255 μL in a standard 3 mm NMR tube for a final concentration of 1.5 mM. The membrane mimicking sample was prepared by dissolving 3.5 mg of peptide H1 in a buffer solution containing 20.6 mg of dDPC and 1.8 mg of dSDS and 10% (v/v) D_2O for a total volume of 400 μL. The concentration of peptide H1 (2.7 mM) and detergents (162 mM) were defined in order to conserve a peptide/micelle ratio of 1/1 according the aggregation number 60 of DPC. In order to have a homogeneous mixture of micelles and peptide,

the sample was submitted to 5 freeze/thaw cycles and transferred to a standard 3 mm NMR tube. The pH 6.8 was checked directly in NMR tube using a PH 211 microprocessor pH meter (Hanna® instruments).

All NMR spectra were acquired on Bruker® Advance 700 MHz NMR spectrometer equipped by a TXI triple resonance $^{1}H/^{15}N/^{13}C/^{2}H$ and z-axis gradient standard probe. Chemical shifts were referenced relative to internal H_2O. The 1D 1H NMR experiments were acquired at 300 K using excitation sculpting with gradients for water suppression [40]. Two-dimensional NOESY and TOCSY using the same water suppression sequence for the two samples, [41] were acquired at the same temperature and a mixing time of 250 ms for the NOESY and a spinlock of 90 ms for the TOCSY. All spectra were processed using the standard programs TopSpin 3.2 (Bruker®), and displayed using Ccpnmr Analysis [42]. Both amide and alpha protons chemical shifts were manually assigned from 2D homonuclear $^{1}H–^{1}H$ NOESY and TOCSY spectra. The NOESY experiment provides both the interconnectivity of the amino acids and the inherent local structuration of the peptide by revealing spatial interatomic distances between pairs of protons for distances shorter than 6 Å. The chemical shift was then used to determine φ and ψ angle and the secondary structure of the peptide using the software DANGLE (Nicole Cheung, Tim Stevens, Bill Broadhurst, University of Cambridge). The helical wheel projection was displayed using Heliquest web tool [43]. A manual assignment was produced following well known protocols based on amide and alpha protons sequential interconnectivities (NHi NHi + 1). The 2D TOCSY spectrum was used to unambiguously assign some peak profiles to a specific amino acid and corroborate the sequential assignment of all amino acids in the peptide.

3. Results and discussion

3.1. Study of the human TRPA1 C-terminal region propensity for membrane interaction

The whole C-terminus of human TRPA1 protein (I957–P1119, IGLAVGDIAEVQKHASLKRIAMQVELHTSLEKKLPLWFLRKVDQKSTIVYPNK PRSGGMLFHIFCFLFCTGEIRQEIPNADKSLEMEILKQKYRLKDLTFLLEKQHEL IKLIIQKMEIISETEDDDSHCSFQDRFKKEQMEQRNSRWNTVLRAVKAKTHH LEP, GenBank® accession number NM_007332) was tested for prediction of antibacterial activity with AntiBP Server (http://www.imtech.res.in/cgibin/antibp/antibp1.pl). Prediction was done by using SVM based method [26]. As mentioned in the introduction, the idea behind is that potential membrane interaction regions of the C-terminus region of TRPA1 should resemble potential antimicrobial peptides. Indeed membrane interaction of both molecules should be ruled by similar properties, mainly electrostatic interactions between basic residues in the peptide and anionic lipids in the membrane.

Prediction results (Table 1) indicate a high propensity for membrane-active regions in the predicted two long and four short α-helices and in adjacent regions bearing positively charged residues in the C-terminus of human TRPA1 [25]. The first proximal part of the C-terminus of human TRPA1 channel was predicted to form a long α-helix and contains several basic amino acid residues which govern voltage and chemical sensitivity of the ion channel protein [25]. Since this domain is assumed to be situated in the immediate vicinity of the cytosolic leaflet of the lipid membrane, it was chosen as the peptide sequence for membrane interaction potential in the present study.

A peptide was synthesized corresponding to the predicted first C-terminal helix of TRPA1 (H1, I964–L992, IAEVQKHASLKRIAMQVELHTSLEKKLPL), and its interaction with model membranes of various lipid composition (zwitterionic, anionic, PIP_2) was studied by differential scanning calorimetry, plasmon waveguide resonance, circular dichroism spectroscopy, attenuated total reflexion infrared spectroscopy, and nuclear magnetic resonance spectroscopy.

Table 1
Mapping of antibacterial peptides within the C-terminus of human TRPA1 channel protein sequence performed by AntiBP Server.

Peptide	Start position	Score
FHIFCFLFCTGEIRQ	61	1.477
TVLRAVKAKTHHLEP	149	1.178
RWNTVLRAVKAKTHH	146	1.046
HTSLEKKLPLWFLRK	27	0.861
GDIAEVQKHASLKRI	6	0.712
IVYPNKPRSGGMLFH	48	0.659
DIAEVQKHASLKRIA	7	0.598
VGDIAEVQKHASLKR	5	0.542
VYPNKPRSGGMLFHI	49	0.490
DRFKKEQMEQRNSRW	133	0.465
RNSRWNTVLRAVKAK	143	0.394
ILKQKYRLKDLTFLL	88	0.376
MEILKQKYRLKDLTF	86	0.358
LEMEILKQKYRLKDL	84	0.350
QRNSRWNTVLRAVKA	142	0.350
IFCFLFCTGEIRQEI	63	0.347
QMEQRNSRWNTVLRA	139	0.263
FLRKVDQKSTIVYPN	38	0.251
GGMLFHIFCFLFCTG	57	0.246
NKPRSGGMLFHIFCF	52	0.233
KSTIVYPNKPRSGGM	45	0.151
VDQKSTIVYPNKPRS	42	0.118
TIVYPNKPRSGGMLF	47	0.110
EVQKHASLKRIAMQV	10	0.079
DSHCSFQDRFKKEQM	126	0.060
DDDSHCSFQDRFKKE	124	0.036

Note: All peptides showed antibacterial potential.

3.2. The effect of H1 on membrane integrity and lipid phase transition

Calcein leakage assays were performed with POPC, POPA, POPS and POPG liposomes in presence of H1 at P/L ratios of 1/50 and 1/25. No leakage was observed with any of the lipids, indicating that this peptide does not perturb the membrane integrity (e.g. pore formation) (data not shown).

The effect of the peptide on the lipid phase transition of DMPC, DMPG, DMPS and DMPA and the binary lipid mixtures of DMPG/DMPS (1/1 mol/mol), DMPG/DMPA (1/1 mol/mol), and DMPA/DMPS (1/1 mol/mol) were investigated by DSC. By following changes in the pre-transition (Lβ′ to the Pβ′) and main transition (Pβ′ to Lα) temperature and enthalpy, information about the mode of interaction and lipid effect on the lipid headgroup and fatty acid chain regions can be obtained (such as effects in the headgroup tilting, cooperativity of the transition and membrane fluidity). One should refer that DSC studies are usually performed with lipids whose phase transition temperature is around room temperature and in any case the phase transition temperature can be outside the measurable instrument range (0–100 °C). In the present study dimyristoyl (DM) fatty acid chain lipids where used because these lipids meets the above mentioned criteria. The data indicates that H1 does not affect the Tm and slightly affects the enthalpy of DMPC main phase transition with a decrease in the cooperativity of the transition (Fig. 1, Table 2). This indicates that the peptide does not strongly perturb the fatty acid chain packing so it does not deeply insert into the lipid hydrophobic core of DMPC. In the case of the anionic lipids DMPG, DMPS and DMPA the scenario is quite different, the peptide strongly affects both the Tm and the enthalpy of the transition that is almost abolished in the case of DMPG at P/L 1/10. This indicates that H1 is strongly perturbing and disrupting the fatty acid chain packing of these lipids. The reduction in ΔH follows the sequence: PG (~90%) > PS (~50%) > PA (~40%). H1 effect on the Tm of anionic lipid is very different, with a decrease in Tm for PG and an increase for PS and PA. This indicates that H1 leads to an increase in membrane fluidity of PG and a decrease for PS and PA, therefore it inserts and perturbs differently PG and PS or PA. Such headgroup specific behavior has been observed for the interaction of other peptides with

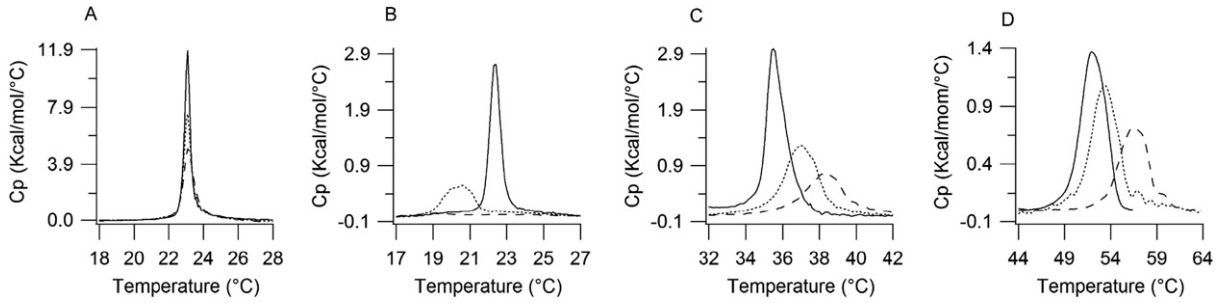

Fig. 1. High-sensitivity DSC heating scans illustrating the effect of the addition of increasing quantities of H1 peptide on the thermotropic phase behavior of DMPC (A), DMPG (B), DMPS (C) and DMPA (D) multilamellar vesicles. The solid line corresponds to the lipid alone and dotted and dashed lines correspond to peptide addition and P/L ratio of 1/50 and 1/25 respectively. Thermodynamic parameters are given in Table 1.

membranes such as the case of protegrin-1 where calorimetry studies have evidenced a headgroup specific behavior for interaction with anionic lipids [44].

For the binary lipid mixtures composed of equimolar amounts of two anionic lipids (DMPG/DMPS, DMPG/DMPA and DMPS/DMPA), the rationale behind such experiment was to investigate if the peptide H1 would selectively affect one of the two lipids in the mixture. Such analysis is possible because each lipid has a sufficiently different Tm that allows it to be identified in the mixture but not too different so that the mixture is still miscible (the general rule being that lipids with Tm farther apart than ~40 °C are not miscible) [45]. H1 leads to an increase in Tm for all binary lipid compositions, the lowest effect being on DMPG/DMPS with an increase of about 2.4 °C in Tm, an intermediate effect for DMPG/DMPA with an increase of 3.6 °C and the highest effect in DMPS/DMPA with an increase of 5.3 °C in Tm (Table 1 in SI). If one compares H1 effect on the binary lipid mixtures compared to the single lipids, one can observe that the effect is not simply additive (an average of the effect observed on the two lipids alone). In the two mixtures containing PG (PG/PS and PG/PA) there is an increase in Tm since PG alone leads to a decrease in Tm, this indicates that PS and PA in these mixtures is the main contributor to the response. Additionally, for the PS/PA mixture the peptide response is increased when compared to each lipid alone. This will be further discussed in the next section, in the context of the binding affinity of H1 and effect on lipid organization.

Relative to the decrease in ΔH following H1 addition, the larger decrease was observed in the two mixtures containing PG (about 42% and 36% decrease for PG/PS and PG/PA, respectively) and the lowest decrease was observed for PA/PS (~16%). The decrease in enthalpy indicates that the peptide perturbs the fatty acid chain packing of these lipids due to its intercalation, the perturbation being greater when PG is present.

Table 2
Thermodynamic parameters obtained by DSC for the interaction of H1 with MLVs composed of DMPC, DMPG, DMPS and DMPA at P/L ratios of 1/50 and 1/25.

Lipid	P/L	T_m (°C)	ΔH_m (kcal/mol)	$\Delta T_{½}$(°C)
DMPC	0	23.1	6.7	0.4
	1/50	23.1	5.7	0.5
	1/25	23.1	5.3	0.7
DMPG	0	22.4	6.3	0.7
	1/50	20.6	3.3	1.9
	1/25	19.2	0.7	2.2
DMPS	0	35.5	5.1	1.1
	1/50	37.0	3.3	2.0
	1/25	38.4	2.5	2.5
DMPA	0	52.0	4.9	3.2
	1/50	53.5	4.3	3.5
	1/25	56.3	3.0	3.6

3.3. Binding affinity of H1 for lipids and effects on lipid membrane anisotropy

The interaction of H1 peptide with planar solid-supported lipid bilayers composed of varied lipid composition was monitored by PWR. For all the lipid compositions, H1 addition to the membrane leads to shifts in the resonance angle position (no changes in the TIR angle at the investigated concentrations) (Table 2 in SI). Since no changes in resonance where observed when H1 was added to the PWR cell (at similar concentrations) in absence of lipid bilayer this means that the observed lipid interactions are specific. Fig. 2 panels A and B represent such spectral changes for the formation of a lipid bilayer made of POPS and subsequent H1 interaction at saturating concentrations. Such spectral changes can be due to mass change induced by the peptide itself and/or lipid reorganization to accommodate such interaction (in those experiments we cannot discriminate between the two possibilities). In all cases from the analysis of the changes in the minimum position for incremental addition of peptide, dissociation constants for the peptide/lipid interaction where determined (Fig. 2, panel C; detailed information can be found in Materials and Methods). An affinity from the low to the high nanomolar range was observed for the lipid mixtures investigated, the affinity being the lowest for the zwitterionic lipid POPC (~480 nM) and the highest for the anionic lipid POPS (7 nM) (Table 3). The results indicate that electrostatic interactions between the peptide and the lipid are important but not essential for the binding. Moreover, the affinity for different anionic lipids (PG, PA and PS) is significantly distinct which indicates a certain level of specificity in those interactions. Interestingly the highest affinity is observed for PS, a lipid that is highly present in the internal leaflet of mammalian cells [28,29,46] where the peptide H1 is prone to interact. Taking into account the composition of the internal leaflet of the membrane and the growing reported importance of PIP_2 in regulation of ion channel function [20–22,47–50], we have also looked at the interaction of H1 with a POPC membrane containing 5% of PIP_2 (usual maximal concentration found in the membrane internal leaflet). The presence of PIP_2 in the POPC membrane increased the affinity of the H1 peptide to the membrane (from 480 to 73 nM), showing the importance of this lipid. Considering the important role of Ca^{2+} in the regulation of TRPA1 channel activity [51–55], this ion was added to the buffer used in these experiments (2 mM). The presence of Ca^{2+} reduced the affinity of the peptide for all the lipids except for POPC. Strong electrostatic interaction of calcium ions with anionic lipid headgroups has been well documented in literature [56–59] therefore the decrease in affinity observed here should result from simple competition between calcium ions and peptide for interaction with the anionic headgroups.

As for the direction of the resonance shifts induced by the peptide, mostly positive spectral shifts were induced by the peptide, except for POPG lipid (Table 2 in SI). Positive spectral changes for both polarizations are mainly correlated with an increase in the mass of the system

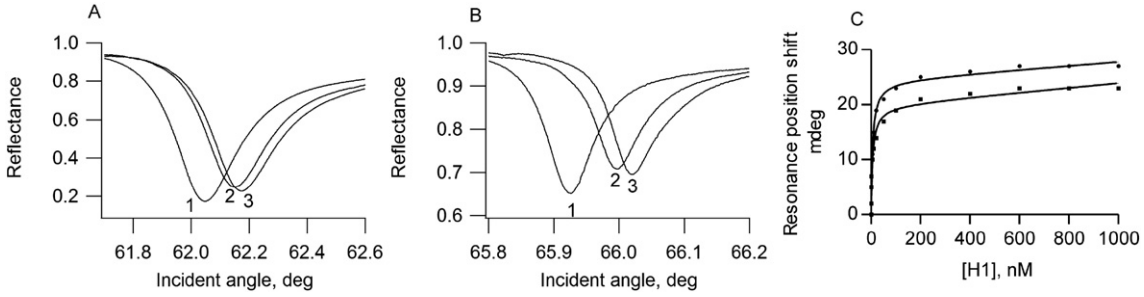

Fig. 2. Interaction of H1 peptide with a POPS planar solid-supported membrane investigated by PWR. PWR spectral shifts observed for buffer (1) after formation of a POPS membrane (2) and following saturating addition of H1 (3) (1 μM) obtained with the *p*- (panel A) and *s*- (panel B) polarized light. Binding curve for H1 interaction with POPS with *p*- (•) and *s*-polarized light (■) (panel C).

due to peptide adsorption. This may or not be accompanied by reorganization in the lipid bilayer, in this case the positive spectral shifts observed (larger for *p*- than *s*-pol) can be explained by an increase in the packing and lipid ordering (decrease in the area per lipid). This can be the case here because the shifts in *p*-pol are larger than in *s*-pol, indicating an increase in ordering resulting in a high packing of the membrane. In the case of POPG, a negative shift is observed for both polarizations. Since peptide addition by itself can only result in a mass increase in the membrane, such negative shifts (decrease in mass) can only arise from lipid reorganization to accommodate H1. A decrease in mass of the membrane can result from lipids being removed from the membrane (e.g. detergent effect of some peptides or pore formation) or from a decrease in the lipid chain packing (decrease in the mass density of the membrane). Since calcein leakage experiments indicate that H1 does not lead to membrane leakage, the first hypothesis is refused.

Such results correlate well with calorimetry data that shows that H1 leads to an increase in the phase transition temperature (Tm) of all lipids investigated except PG. Such increase in Tm indicates that H1 disfavors the gel/fluid phase transition or in other words rigidifies the membrane. This agrees well with the increase in mass and lipid packing inferred from PWR data. In the case of PG, the decrease in mass observed by PWR results from a decrease in the lipid packing that agrees with the decrease in Tm and fluidification effect of H1 on PG.

Relative to the magnitude of the spectral changes induced by H1, the values resemble those observed by the interaction of other membrane active peptides with membranes [60,61]. For all lipid systems, shifts observed with *p*-pol were larger than *s*-pol, indicating a certain degree of anisotropy with changes occurring in the perpendicular direction to the membrane being larger than those on the parallel direction (this has been discussed above). The magnitude of the spectral changes was larger for zwitterionic than anionic lipids. Calcium ions had no effect on the magnitude of the spectral changes, only on the affinity.

Table 3
Affinity of H1 to a solid supported lipid bilayer of varied lipid composition in absence and presence of Ca^{2+} in the buffer.

Lipid mixtures	K_D (nM)
POPC	480 ± 59
POPG	82 ± 9
POPS	7 ± 1
POPA	25 ± 5
POPC/PIP_2 5%	73 ± 8
POPC + Ca^{2+}	515 ± 47
POPG + Ca^{2+}	65 ± 7
POPS + Ca^{2+}	47 ± 6
POPA + Ca^{2+}	210 ± 32
POPC/PIP_2 5% + Ca^{2+}	98 ± 12

Note: The buffer used was Tris–HCl 10 mM (pH 7.4), 100 mM NaCl, 2 mM EGTA without or with 2 mM Ca^{2+}.

3.4. Secondary structure of H1 in buffer and upon lipid interaction

CD spectra were recorded to obtain structural information on the peptide both in buffer solution and when bound to vesicles composed of zwitterionic and anionic lipids. All experiments were performed in 10 mM phosphate buffer above the phase transition temperature of the lipids at P/L of 1/25. This is the P/L ratio at which a major effect on the phase transition of the lipids was observed. The CD spectra are presented in Fig. 3. The peptide was unstructured in buffer and also in the presence of zwitterionic lipids (DMPC, POPC, POPE). In the presence of anionic lipids (DMPG, POPG, POPS, POPA), the peptide secondary structure showed major changes. Generally, analysis of CD spectra of H1 peptide in the presence of anionic lipids demonstrated a marked contribution of β-sheet structure. Indeed the percentage of random coil is about 55% and the percentage of β-sheet is about 45% with POPG and POPA. In case of POPS the percentage of random coil is about 60% and the percentage of β-sheet is about 33% with a minor contribution of α-helix (6%). The helical content increases to 23% with DMPG while the percentage of random coil is about 46% and the percentage of β-sheet is about 31%. Thus is seems that the fatty acid chain length also influences the secondary structure adopted by the peptide, shorter fatty acid chains promoting increase in the helical content. The highest structural contribution of β-sheet (about 70%) is found when PIP_2 is present (POPC/PIP_2, 9/1 mol/mol) and the percentage of random coil is about 30%. These results indicate that electrostatic interactions between lipid and peptide as well as lipid specificity govern the conformation change to a β-sheet structure.

In order to elucidate the role of calcium ions in the structural transitions of H1 peptide, Ca^{2+} was added to the buffer used in these experiments (1–2 mM). With POPS liposomes (SI Fig. 1 A) the presence of

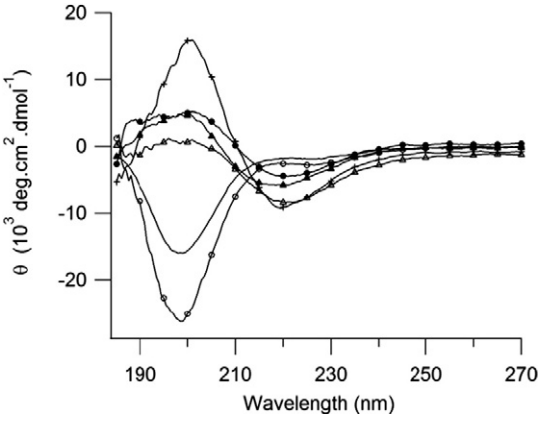

Fig. 3. CD spectra of H1 peptide in phosphate buffer (solid line) and in presence of LUVs (1 mg/mL) of POPC (○), POPG (•), POPC/PIP2 (9/1 mol/mol) (+), POPS (Δ) and POPA (▲).

2 mM Ca^{2+} induces a profound change in the secondary structure of H1, leading to unstructured peptide devoid of any β-sheet content. In contrast, in the presence of DMPG and POPG liposomes (SI Fig. 1 B and C, respectively) the peptide secondary structure does not change significantly after addition of Ca^{2+}. Indeed the percentage of β-sheet is between 40 and 60% in the presence of 2 mM Ca^{2+} with DMPG and POPG, indicating that H1 peptide interacts with anionic lipids in a headgroup-specific manner. These findings were confirmed with different peptide concentrations and P/L ratios (not shown).

With POPC liposomes containing PIP_2 (POPC/PIP_2, 9/1 mol/mol), the structural content of β-sheet after addition of Ca^{2+} was dependent on peptide concentration (SI Fig. 2 A and B). In the presence of 1 mM Ca^{2+}, the peptide is mostly unstructured at a P/L ratio of 1/50, the percentage of random coil is about 93% and the percentage of β-sheet and α-helix is 3–4% (SI Fig. 2 A). In contrast, at a higher peptide concentration, the percentage of random coil is about 80% and the percentage of β-sheet is about 20% with POPC/PIP2 liposomes in the presence of 1 mM Ca^{2+} (SI Fig. 2 B). These results allow the speculation that conformational transitions of the H1 peptide enable this domain to function as a sensor of PIP_2 and Ca^{2+}.

As NMR studies have been performed in presence of SDS and DPC, CD spectra of the peptide in SDS and SDS/DPC (9/1) at a P/L ratio of 1/60 are presented in SI (Fig. 3) and indicate a typical helical signature. It is not clear why the peptides adopt a α-helical structure in presence of SDS and DPC/SDS (9/1 mol/mol) while in presence of anionic lipids a β-sheet structure is predominant. One possibility is that, despite the fact that one is comparing lipids with detergents, the membrane thickness of the two objects is quite different and could affect peptide structure adoption. Indeed, as mentioned above, the helical content increased from about none to 23% when going from POPG (C16, C18) to DMPG (C14). Thus following the same order, one would except that for DPC (C12) the helical content would increase which was the case. To test this hypothesis, the DPC/SDS micelles were doped with POPC (10 mg, 33 mM) and the NMR spectra acquired. Even though no attributions were possible with this sample as objects become large and in the limit of NMR resolution, there was a marked decrease of helical structure (data not shown). This is in agreement with the hypothesis that longer lipid chains induce lost of helical structure. The part that remained helical was still visualized by the 2D NMR spectra and comprised residues 1 to 7.

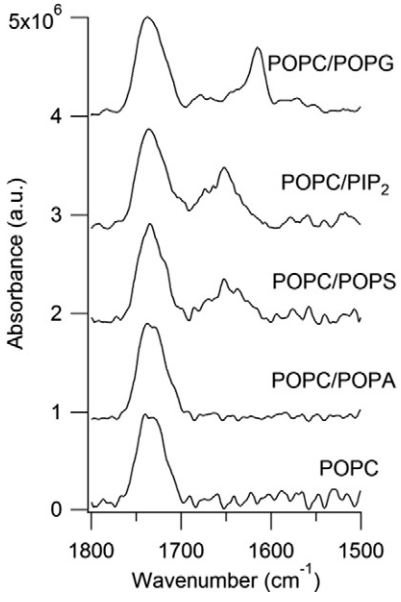

Fig. 4. p-polarized ATR-FTIR spectra of H1 in presence of different lipid bilayer used as membrane model in D_2O. From bottom to top, pure POPC membrane, mixture POPC-POPA (7/3 mol/mol), mixture POPC/POPS (7/3 mol/mol), mixture POPC/PIP2 (9/1 mol/mol) and mixture POPC/POPG (7/3 mol/mol). For all the spectra baseline subtraction were performed, the spectra were normalized on the band at 1740 cm^{-1} ($\nu C=O$ of the phospholipid).

Polarized ATR-FTIR experiments were performed to evaluate the structure of H1 interacting with the various model membranes. Lipid bilayers were formed by the fusion of SUVs onto the ATR germanium crystal. The formation and the organization of the bilayer was monitored by the dichroic ratio (R_{ATR}) of the ν_{as} (CH_2 — 2923 cm^{-1}) and ν_s (CH_2 — 2853 cm^{-1}) band of the lipid chain (Fig. 4 in SI), as described by Castano and Desbat [39]. The protein H1 (1 mM) was added to lipids and incubated (10 min at room temperature after which the ATR cell was rinsed with D_2O avoiding the exposure to air. The H/D exchange leads to a better observation of amide I band and the determination of the secondary structures of the peptides, however due to this exchange the amide II band is shifted to lower wavenumber around 1450 cm^{-1}. The ATR-FTIR spectra were recorded with *s*- and *p*-polarization. Fig. 4 shows the *p*-polarized ATR-FTIR spectra of H1 bound to membrane. The band at 1740 cm^{-1} band is assigned to the C═O stretching mode of the phospholipids. No significant binding of H1 was observed on the pure POPC membrane, in agreement with the lowest affinity constant determined by PWR. Similar result was obtained with the mixture POPC-POPA (7/3). A broad amide I band was observed for H1 interacting with POPC-POPS (7/3) membrane revealing the presence of different secondary structure**s** for H1. The absorbance is weak and due to the presence of TFA (at 1670 cm^{-1}) in the sample a decomposition of the amide I band cannot be performed. Including PIP_2 (POPC/PIP_2, 9/1 mol/mol) in POPC favors the interaction of H1 with the membrane, a broad amide I′ band was observed on the ATR-FTIR spectrum (Fig. 4). As previously described the broad band indicates preferentially various secondary structure**s** for the H1 bound to the membrane. H1 interacting with POPC-POPG (7/3) membrane induces a large modification of the shape of amide I band. The band is mainly at 1615 cm^{-1} with a small contribution at around 1685 cm^{-1}. These bands are characteristics of an antiparallel β-sheet organization [62–64]. The 30% of POPG leads to a large structuration of the H1 peptide.

However, whatever the studied membrane, no significant difference was observed for the dichroic ratio (R = Ap/As), comparing the spectra in presence or in absence of the H1 (Fig. 4 in SI). Thus, the organization of the membrane is poorly affected by the binding of H1, excluding a strong insertion of H1 in the lipid bilayer and there is no preferential orientation of H1 on the membrane.

3.5. Folding of H1 peptide in membrane model systems followed by NMR spectroscopy

NMR spectroscopy was used to monitor the structural changes of H1 peptide from an aqueous solution to a membrane model environment. Due to the important loss of tumbling in the NMR time scale for H1 peptide in membranes composed of phospholipids such as POPG, POPC or DMPG, small micelles composed of mixtures of LMPG and DPC/SDS (10% SDS) were chosen for NMR studies. Yet, LMPG membrane models in presence of peptide are not ideal, since from the NMR 2D spectra a very limit number of peaks and all very broad were observed, indicating a tumbling rate out of the suited range for solution NMR experiments. Therefore, NMR studies were performed in presence of SDS and DPC, which enable a much better acquisition of 2D spectra. The peptide secondary structure was investigated by CD spectroscopy prior to the NMR measurements (as described above). DPC has been used in several examples as a simpler membrane model that is more compatible with NMR (as an example see [65]). In buffer solution the ^1H–^1H NOESY spectra of H1 peptide (Fig. 5, purple contours) shows a typical pattern of a random coil with most αH–NH connectivities collapsed in a small region (7.5–8.5 ppm). In addition a much lower number of H–H connectivities are observed in the entire spectrum. Once the peptide is transferred to PC/SDS mixtures, the number of αH–NH and NH–NH cross peaks increases and spread over a much larger chemical shift range indicating the formation of a structured

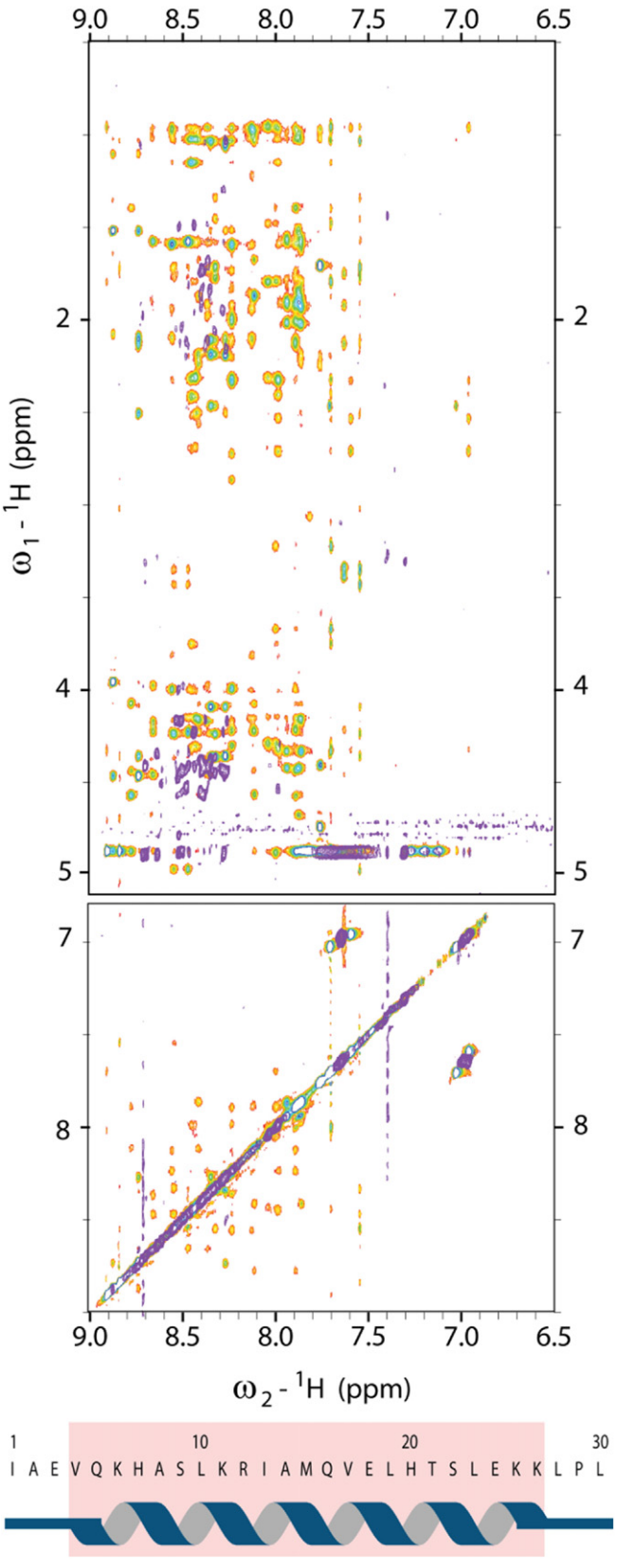

Fig. 5. ^{1}H–^{1}H NOESY NMR spectra of peptide A1 in solution and in membrane mimicking interface, purple and red-orange-green contours, respectively. The spectra shows the formation of a helical structure once the peptide is immersed in DPC:SDS (9:1) micelles. The 2D NOESY zoom in the spectra clearly shows the formation of N–H–NH short and i + 3 and i + 4 connectivities that together with αH–NH crosspeaks characterize the α-helical projection (bottom).

peptide (orange-green spectra). The determination of the degree of folding was addressed by using the differences between the observed amide chemical shift coefficients and random coil values (delta HN). The result of this analysis is plotted in Fig. 5 indicating that most of the peptide forms a α-helix when in contact with negatively charged micelles (see also Fig. 5 in SI). It should be noted that the helical part spans over 25–27 residues, which is larger than the minimal amount of residues necessary to span a typical cellular membrane, e.g., 20–21 residues. The results are contrasting with the secondary structure observed by CD and IR in anionic liposomes and flat membranes. Besides the fact that the fatty acid chain length may influence the peptide structural changes, shorter chains promoting helical structure (as described in the CD section above), it should also be pointed out that the size of the micelles used in NMR are way smaller than LUVs (1–5 nm *vs* 100 nm, respectively). Therefore the surface presented to the peptide in the case of detergent micelles is very small and so the peptide cannot interact superficially as in the case of LUVs (CD studies) and flat membranes (IR studies). In micelles the peptide is probably located in the center of the micelle which forces it to adopt a different secondary structure.

4. Conclusions

The studies performed have clearly shown that the H1 peptide, corresponding to the first putative membrane interaction region in the C-terminus of TRPA1 channel, interacts with lipid membrane model systems. A marked interaction and increased affinity is observed for membranes containing anionic lipids. The peptide also changes its secondary structure from random to mostly β-sheet upon contact with anionic membranes. The study reveals that the anionic character of the membrane is important for the P/L interaction. Moreover, the mode of interaction with the lipid membrane is also headgroup specific as both the affinity, the effect in membrane fluidity and peptide secondary structure adopted is rather different between PS, PG and PIP_2 containing membranes.

Other ion channels' activity has been shown to be highly modulated by the lipid environment not only indirectly by the collective physical properties of the membrane, but by direct interactions of lipids, especially anionic ones through specific basic amino acids in the protein. Phosphoinositides and in particularly PIP_2 have been shown to regulate almost every class of ion channel [47–49]. Indeed, in the case of the potassium channel (Kir), anionic lipids would act very much like pre-localized ligands being able to induce quite rapid gating motions in the channel, considerably faster than classical ligands that would need to diffuse to the channel binding site to exert their action [66].

The fact that the affinity of H1 to PIP_2 containing membranes is quite high and enhanced relative to other lipids suggests that important electrostatic interactions occur between the peptide H1 (comporting 5 basic residues) and the negatively charged lipid headgroup. The idea that electrostatic interactions are important for the P/L interaction is reinforced by the fact that Ca^{+2} ions in the medium decrease the binding of H1 to all the anionic lipids. Therefore, the TRPA1 channel could, like other channels use this membrane binding sites in the C-terminal region to modulate its conformational change, activity and gating properties.

Many questions remain yet open, including the nature of the conformational changes induced by anionic lipid interaction, whether the lipid binding will activate or inhibit the channel (as both cases have been observed depending on the channel) and the physiological relevance of such regulation. It also remains to be investigated whether the other putative membrane interacting domains in the C-terminal region of TRPA1 share the same membrane interaction properties.

Transparency document

The Transparency document associated with this article can be found, in online version.

Acknowledgements

This work was supported by Ministry of Education, Youth and Sports of the Czech Republic Grant OP VK CZ.1.07/2.3.00/30.0025.

Appendix A. Supplementary data

Supplementary data to this article can be found online at http://dx.doi.org/10.1016/j.bbamem.2015.02.003.

References

[1] D.E. Clapham, TRP channels as cellular sensors, Nature 426 (2003) 517–524.
[2] L.J. Wu, T.B. Sweet, D.E. Clapham, International Union of Basic and Clinical Pharmacology. LXXVI. Current progress in the mammalian TRP ion channel family, Pharmacol. Rev. 62 (2010) 381–404.
[3] M. Sisignano, D.L. Bennett, G. Geisslinger, K. Scholich, TRP-channels as key integrators of lipid pathways in nociceptive neurons, Prog. Lipid Res. 53 (2014) 93–107.
[4] S. Bang, S. Yoo, U. Oh, S.W. Hwang, Endogenous lipid-derived ligands for sensory TRP ion channels and their pain modulation, Arch. Pharm. Res. 33 (2010) 1509–1520.
[5] B. Nilius, G. Owsianik, T. Voets, J.A. Peters, Transient receptor potential cation channels in disease, Physiol. Rev. 87 (2007) 165–217.
[6] M. Bodding, TRP proteins and cancer, Cell. Signal. 19 (2007) 617–624.
[7] J. Garcia-Anoveros, K. Nagata, Trpa1, Handb Exp Pharmacol (2007) 347–362.
[8] B. Nilius, G. Appendino, G. Owsianik, The transient receptor potential channel TRPA1: from gene to pathophysiology, Pflugers Arch. 464 (2012) 425–458.
[9] Y. Dai, S. Wang, M. Tominaga, S. Yamamoto, T. Fukuoka, T. Higashi, K. Kobayashi, K. Obata, H. Yamanaka, K. Noguchi, Sensitization of TRPA1 by PAR2 contributes to the sensation of inflammatory pain, J. Clin. Invest. 117 (2007) 1979–1987.
[10] Y. Karashima, J. Prenen, V. Meseguer, G. Owsianik, T. Voets, B. Nilius, Modulation of the transient receptor potential channel TRPA1 by phosphatidylinositol 4,5-biphosphate manipulators, Pflugers Arch. 457 (2008) 77–89.
[11] D. Kim, E.J. Cavanaugh, D. Simkin, Inhibition of transient receptor potential A1 channel by phosphatidylinositol-4,5-bisphosphate, Am. J. Physiol. Cell Physiol. 295 (2008) C92–C99.
[12] S.J. Tucker, T. Baukrowitz, How highly charged anionic lipids bind and regulate ion channels, J. Gen. Physiol. 131 (2008) 431–438.
[13] J.A. Poveda, A.M. Giudici, M.L. Renart, M.L. Molina, E. Montoya, A. Fernandez-Carvajal, G. Fernandez-Ballester, J.A. Encinar, J.M. Gonzalez-Ros, Lipid modulation of ion channels through specific binding sites, Biochim. Biophys. Acta 1838 (2014) 1560–1567.
[14] J. Chemin, A.J. Patel, F. Duprat, I. Lauritzen, M. Lazdunski, E. Honore, A phospholipid sensor controls mechanogating of the K^+ channel TREK-1, EMBO J. 24 (2005) 44–53.
[15] D. Enkvetchakul, I. Jeliazkova, J. Bhattacharyya, C.G. Nichols, Control of inward rectifier K channel activity by lipid tethering of cytoplasmic domains, J. Gen. Physiol. 130 (2007) 329–334.
[16] G. Sandoz, S.C. Bell, E.Y. Isacoff, Optical probing of a dynamic membrane interaction that regulates the TREK1 channel, Proc. Natl. Acad. Sci. U. S. A. 108 (2011) 2605–2610.
[17] T. Rohacs, C.M. Lopes, I. Michailidis, D.E. Logothetis, PI(4,5)P2 regulates the activation and desensitization of TRPM8 channels through the TRP domain, Nat. Neurosci. 8 (2005) 626–634.
[18] B. Nilius, F. Mahieu, J. Prenen, A. Janssens, G. Owsianik, R. Vennekens, T. Voets, The Ca^{2+}-activated cation channel TRPM4 is regulated by phosphatidylinositol 4,5-biphosphate, EMBO J. 25 (2006) 467–478.
[19] S. Brauchi, G. Orta, M. Salazar, E. Rosenmann, R. Latorre, A hot-sensing cold receptor: C-terminal domain determines thermosensation in transient receptor potential channels, J. Neurosci. 26 (2006) 4835–4840.
[20] T. Rohacs, Regulation of TRP channels by PIP(2), Pflugers Arch. 453 (2007) 753–762.
[21] T. Voets, B. Nilius, Modulation of TRPs by PIPs, J. Physiol. 582 (2007) 939–944.
[22] B. Nilius, G. Owsianik, T. Voets, Transient receptor potential channels meet phosphoinositides, EMBO J. 27 (2008) 2809–2816.
[23] E. Cao, J.F. Cordero-Morales, B. Liu, F. Qin, D. Julius, TRPV1 channels are intrinsically heat sensitive and negatively regulated by phosphoinositide lipids, Neuron 77 (2013) 667–679.
[24] V. Lukacs, J.M. Rives, X. Sun, E. Zakharian, T. Rohacs, Promiscuous activation of transient receptor potential vanilloid 1 (TRPV1) channels by negatively charged intracellular lipids: the key role of endogenous phosphoinositides in maintaining channel activity, J. Biol. Chem. 288 (2013) 35003–35013.
[25] A. Samad, L. Sura, J. Benedikt, R. Ettrich, B. Minofar, J. Teisinger, V. Vlachova, The C-terminal basic residues contribute to the chemical- and voltage-dependent activation of TRPA1, Biochem. J. 433 (2011) 197–204.
[26] S. Lata, B.K. Sharma, G.P. Raghava, Analysis and prediction of antibacterial peptides, BMC Bioinf. 8 (2007) 263.
[27] R.E. Hancock, H.G. Sahl, Antimicrobial and host-defense peptides as new anti-infective therapeutic strategies, Nat. Biotechnol. 24 (2006) 1551–1557.
[28] P.A. Janmey, P.K. Kinnunen, Biophysical properties of lipids and dynamic membranes, Trends Cell Biol. 16 (2006) 538–546.
[29] G. van Meer, D.R. Voelker, G.W. Feigenson, Membrane lipids: where they are and how they behave, Nat. Rev. Mol. Cell Biol. 9 (2008) 112–124.
[30] K. Matsuzaki, Control of cell selectivity of antimicrobial peptides, Biochim. Biophys. Acta 1788 (2009) 1687–1692.
[31] G. Rouser, S. Fkeischer, A. Yamamoto, Two dimensional then layer chromatographic separation of polar lipids and determination of phospholipids by phosphorus analysis of spots, Lipids 5 (1970) 494–496.
[32] Z. Salamon, H.A. Macleod, G. Tollin, Coupled plasmon-waveguide resonators: a new spectroscopic tool for probing proteolipid film structure and properties, Biophys. J. 73 (1997) 2791–2797.
[33] I.D. Alves, C.K. Park, V.J. Hruby, Plasmon resonance methods in GPCR signaling and other membrane events, Curr. Protein Pept. Sci. 6 (2005) 293–312.
[34] E. Harte, N. Maalouli, A. Shalabney, E. Texier, K. Berthelot, S. Lecomte, I.D. Alves, Probing the kinetics of lipid membrane formation and the interaction of a nontoxic and a toxic amyloid with plasmon waveguide resonance, Chem. Commun. (Camb.) 50 (2014) 4168–4171.
[35] P. Mueller, D.O. Rudin, Resting and action potentials in experimental bimolecular lipid membranes, J. Theor. Biol. 18 (1968) 222–258.
[36] Z. Salamon, D. Huang, W.A. Cramer, G. Tollin, Coupled plasmon-waveguide resonance spectroscopy studies of the cytochrome b6f/plastocyanin system in supported lipid bilayer membranes, Biophys. J. 75 (1998) 1874–1885.
[37] I.D. Alves, Z. Salamon, E. Varga, H.I. Yamamura, G. Tollin, V.J. Hruby, Direct observation of G-protein binding to the human delta-opioid receptor using plasmon-waveguide resonance spectroscopy, J. Biol. Chem. 278 (2003) 48890–48897.
[38] E. Goormaghtigh, V. Raussens, J.M. Ruysschaert, Attenuated total reflection infrared spectroscopy of proteins and lipids in biological membranes, Biochim. Biophys. Acta 1422 (1999) 105–185.
[39] S. Castano, B. Desbat, Structure and orientation study of fusion peptide FP23 of gp41 from HIV-1 alone or inserted into various lipid membrane models (mono-, bi- and multibi-layers) by FT-IR spectroscopies and Brewster angle microscopy, Biochim. Biophys. Acta 1715 (2005) 81–95.
[40] T.L. Hwang, Water suppression that works. Excitation sculpting using arbitrary wave-forms and pulsed-field gradients, J. Magn. Reson., Ser. A 112 (1995) 275–279.
[41] M. Piotto, V. Saudek, V. Sklenar, Gradient-tailored excitation for single-quantum NMR spectroscopy of aqueous solutions, J. Biomol. NMR 2 (1992) 661–665.
[42] W.F. Vranken, W. Boucher, T.J. Stevens, R.H. Fogh, A. Pajon, M. Llinas, E.L. Ulrich, J.L. Markley, J. Ionides, E.D. Laue, The CCPN data model for NMR spectroscopy: development of a software pipeline, Proteins 59 (2005) 687–696.
[43] R. Gautier, D. Douguet, B. Antonny, G. Drin, HELIQUEST: a web server to screen sequences with specific alpha-helical properties, Bioinformatics 24 (2008) 2101–2102.
[44] W. Jing, E.J. Prenner, H.J. Vogel, A.J. Waring, R.I. Lehrer, K. Lohner, Headgroup structure and fatty acid chain length of the acidic phospholipids modulate the interaction of membrane mimetic vesicles with the antimicrobial peptide protegrin-1, J. Pept. Sci. 11 (2005) 735–743.
[45] W. Curatolo, B. Sears, L.J. Neuringer, A calorimetry and deuterium NMR study of mixed model membranes of 1-palmitoyl-2-oleylphosphatidylcholine and saturated phosphatidylcholines, Biochim. Biophys. Acta 817 (1985) 261–270.
[46] J.E. Vance, R. Steenbergen, Metabolism and functions of phosphatidylserine, Prog. Lipid Res. 44 (2005) 207–234.
[47] D.W. Hilgemann, S. Feng, C. Nasuhoglu, The complex and intriguing lives of PIP2 with ion channels and transporters, Sci. STKE 2001 (2001) re19.
[48] N. Gamper, M.S. Shapiro, Regulation of ion transport proteins by membrane phosphoinositides, Nat. Rev. Neurosci. 8 (2007) 921–934.
[49] B.C. Suh, B. Hille, PIP2 is a necessary cofactor for ion channel function: how and why? Annu. Rev. Biophys. 37 (2008) 175–195.
[50] A.A. Rodriguez-Menchaca, S.K. Adney, L. Zhou, D.E. Logothetis, Dual regulation of voltage-sensitive ion channels by PIP(2), Front. Pharmacol. 3 (2012) 170.
[51] K. Nagata, A. Duggan, G. Kumar, J. Garcia-Anoveros, Nociceptor and hair cell transducer properties of TRPA1, a channel for pain and hearing, J. Neurosci. 25 (2005) 4052–4061.
[52] J.F. Doerner, G. Gisselmann, H. Hatt, C.H. Wetzel, Transient receptor potential channel A1 is directly gated by calcium ions, J. Biol. Chem. 282 (2007) 13180–13189.
[53] S. Zurborg, B. Yurgionas, J.A. Jira, O. Caspani, P.A. Heppenstall, Direct activation of the ion channel TRPA1 by Ca2+, Nat. Neurosci. 10 (2007) 277–279.
[54] Y.Y. Wang, R.B. Chang, H.N. Waters, D.D. McKemy, E.R. Liman, The nociceptor ion channel TRPA1 is potentiated and inactivated by permeating calcium ions, J. Biol. Chem. 283 (2008) 32691–32703.
[55] L. Sura, V. Zima, L. Marsakova, A. Hynkova, I. Barvik, V. Vlachova, C-terminal acidic cluster is involved in Ca^{2+}-induced regulation of human transient receptor potential ankyrin 1 channel, J. Biol. Chem. 287 (2012) 18067–18077.
[56] D. Papahadjopoulos, Surface properties of acidic phospholipids: interaction of monolayers and hydrated liquid crystals with uni- and bi-valent metal ions, Biochim. Biophys. Acta 163 (1968) 240–254.
[57] J.F. Tocanne, P.H. Ververgaert, A.J. Verkleij, L.L. van Deenen, A monolayer and freeze-etching study of charged phospholipids. II. Ionic properties of mixtures of phosphatidylglycerol and lysylphosphatidylglycerol, Chem. Phys. Lipids 12 (1974) 220–231.
[58] I. Haller, M.J. Freiser, Structural changes in bilayer membranes by multivalent ions, Biochim. Biophys. Acta 455 (1976) 739–748.
[59] U.R. Pedersen, C. Leidy, P. Westh, G.H. Peters, The effect of calcium on the properties of charged phospholipid bilayers, Biochim. Biophys. Acta 1758 (2006) 573–582.
[60] I.D. Alves, I. Correia, C.Y. Jiao, E. Sachon, S. Sagan, S. Lavielle, G. Tollin, G. Chassaing, The interaction of cell-penetrating peptides with lipid model systems and subsequent lipid reorganization: thermodynamic and structural characterization, J. Pept. Sci. 15 (2009) 200–209.

[61] M.L. Jobin, P. Bonnafous, H. Temsamani, F. Dole, A. Grelard, E.J. Dufourc, I.D. Alves, The enhanced membrane interaction and perturbation of a cell penetrating peptide in the presence of anionic lipids: toward an understanding of its selectivity for cancer cells, Biochim. Biophys. Acta 1828 (2013) 1457–1470.
[62] E. Goormaghtigh, V. Cabiaux, J.M. Ruysschaert, Determination of soluble and membrane protein structure by Fourier transform infrared spectroscopy. I. Assignments and model compounds, Subcell. Biochem. 23 (1994) 329–362.
[63] Y.N. Chirgadze, N.A. Nevskaya, Infrared spectra and resonance interaction of amide-I vibration of the antiparallel-chain pleated sheet, Biopolymers 15 (1976) 607–625.
[64] K. Berthelot, H.P. Ta, J. Gean, S. Lecomte, C. Cullin, In vivo and in vitro analyses of toxic mutants of HET-s: FTIR antiparallel signature correlates with amyloid toxicity, J. Mol. Biol. 412 (2011) 137–152.
[65] G.F. Salgado, R. Marquant, A. Vogel, I.D. Alves, S.E. Feller, N. Morellet, S. Bouaziz, Structural studies of HIV-1 Gag p6ct and its interaction with Vpr determined by solution nuclear magnetic resonance, Biochemistry 48 (2009) 2355–2367.
[66] M. Rapedius, P.W. Fowler, L. Shang, M.S. Sansom, S.J. Tucker, T. Baukrowitz, H bonding at the helix-bundle crossing controls gating in Kir potassium channels, Neuron 55 (2007) 602–614.